Effect of Postdrawing on the Permeability of Gases in Blown Polyethylene Film*

JAMES P. PAULOS and EDWIN L. THOMAS,† *Department of Chemical Engineering, University of Minnesota, Minneapolis, Minnesota 55455*

Synopsis

The effect of orientation on the structure and transport properties of high-density polyethylene film has been studied. Microstructure was characterized using small-angle light scattering, birefringence, and wide-angle x-ray scattering. Water vapor and oxygen transmission rates were determined as a function of film draw ratio. The object of the present work is to correlate the effects of postprocessing conditions on the transport properties and morphology of linear polyethylene. High-density spherulitic polyethylene films were produced by blown film extrusion and subsequently oriented by longitudinal stretching in a postoperation. Various degrees of orientation were imparted to the films, with percent crystallinity, sample orientation and transport properties measured as a function of draw ratio. For the postoriented films, results indicate there was no significant change in percent crystallinity with increasing draw ratio although water vapor and oxygen permeability decreased substantially. This is attributed to the increased orientation of the crystalline and amorphous regions and rod-like and microfibril structure formation brought about by the drawing process. Lower processing temperatures result in increased orientation which improves the vapor barrier properties.

INTRODUCTION

Barrier characteristics of films have been previously shown to improve significantly with increasing draw ratio. Semicrystalline as well as amorphous polymers have been shown to exhibit this effect, including polyethylene,[1-3] polypropylene,[1] nylon,[2] poly(vinyl chloride),[1,4] poly(ethylene terephthalate),[1,2,5] and polycarbonate.[6] Lower permeability would be expected for films having a higher degree of crystallinity, which has been reported to be induced in highly drawn samples, since it is the crystalline content which acts as the impermeable component in the film.[7] However, other structural parameter(s) may be responsible for the increased vapor barrier resistance observed, since sample morphology may change without an appreciable change in crystallinity. One possible explanation is that a substantial reduction in the equilibrium sorption and diffusion takes place as a consequence of microfibril formation and the denser packing and the ordering of the tie molecules in the amorphous regions brought about by the drawing process.[8] Consequently, a basic understanding of the structure/transport property relationship in drawn polyethylene film requires a detailed knowledge of the film microstructure and state of orientation.

* Part of Masters of Engineering Thesis (J.P.P.), University of Minnesota.

† Present address: Polymer Science & Engineering, University of Massachusetts, Amherst, Massachusetts.

Journal of Applied Polymer Science, Vol. 25, 15–23 (1980)

0021-8995/80/0025-0015$01.00

EXPERIMENTAL

Preparation and Orientation of Film Samples

The polymer used in this study was a linear, high-density polyethylene having an equilibrium resin density of 0.950 g/cm^3 and melt index of 0.45 measured at 190°C. Film was prepared by the blown film extrusion process as shown schematically in Figure 1. Resin, in pellet form, is fed through the hopper into an extruder. Within the extruder, heat and friction melt the resin, and the polymer is pumped through an annular die. Air pressure inside the film bubble maintains the shape, and cool air is blown on the outside of the bubble to solidify the polymer melt. The film bubble is drawn away from the die as well as blown outward to arrive at the desired gauge and layflat width. The bubble is then flattened by collapsing frames, drawn through nip rolls, slit into sheeting, separated, and wound into finished rolls. All samples were prepared in the manner described using commercial melt extrusion equipment with the use of the same die and extruder.

The blown films were then uniaxially stretched to different draw ratios in a separate postorientation operation, as shown in Figure 2. The roll-to-roll orientation line consists of two sections: (1) preheating and (2) orienting, with separate heat controls for each section.

The preheating section consisted of a pair of heated (127°C) 12 in. (30.5 cm)-diameter polished steel rolls with the film S-wrapped about these rolls. The orientation section (where the stretching is accomplished) has two sets of nip rolls, each consisting of a heated 6 in. (15.25 cm)-diameter polished steel roll and a rubber pressure roll. The speed differential between the two sets of nips was variable from 2:1 to 10:1, to achieve the desired orientation, and the stretch gap between those nips was adjustable from 2.54 × 10^{-2} cm (10 mil) to several centimeters. The draw ratios developed for this study were 4×, 6×, 8×, and 10×.

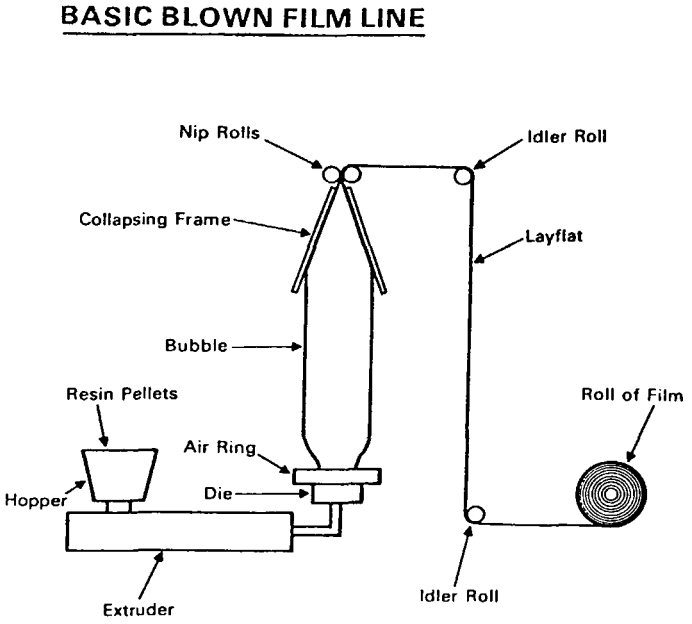

Fig. 1. Schematic of the blown film extrusion process.

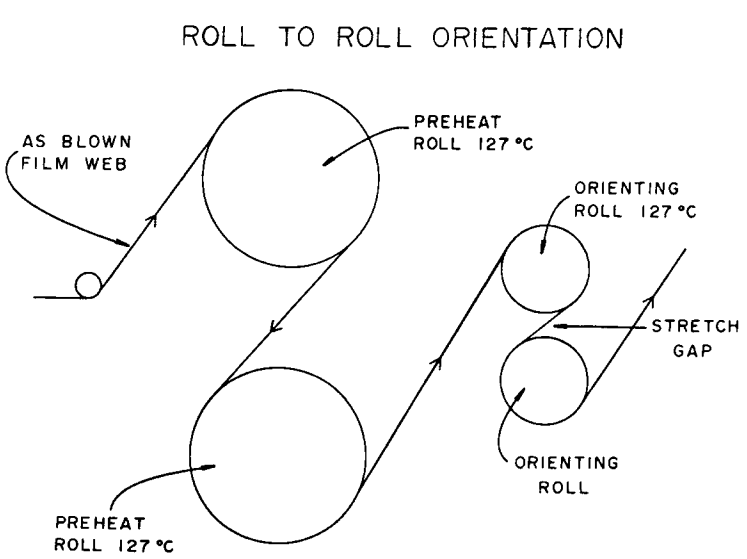

Fig. 2. Schematic of the postorientation of films.

The draw ratio is defined as the reduction in film gauge between input and output rolls, e.g., 0.02-cm film (T_1) fed in with an input speed of 0.3 m/min and output speed of 3 m/min would result in a reduction of film gauge to 0.002 cm (T_2), with a corresponding draw ratio of 10×. Input film gauges and orienting roll speeds were selected to give all the oriented films a final gauge of approximately 2.54×10^{-3} cm (1 mil). Uniaxial orientation was achieved with this equipment by only allowing the film to be stretched over a very small stretch gap (5×10^{-2} cm) which served to minimize transverse contraction.

Morphological Studies

Crystallinity was determined by DSC and density measurements. Heats of fusion were measured on a du Pont model 990 thermal analyzer at a heating rate of 10°C/min with 5-mg samples. The density of the samples was determined using a calibrated density gradient column of isopropyl alcohol–water for densities in the range of 0.89–0.97 g/cm^3.

Small-angle light scattering (SALS) measurements employed a 3-mW helium–neon gas laser with a photographic plate (Polaroid camera) placed behind the analyzer to record the patterns. Patterns were obtained for the case where the polarized incident light and analyzer have their polarization directions perpendicular to one another (designated H_v). For uniaxial deformed samples, the stretch direction (S.D.) is aligned parallel to the plane of polarization of the incident light. The film samples were held between glass microscope slides, and benzoyl alcohol (n = 1.53) was used as an immersion fluid to minimize surface scattering. Overall orientation of the drawn polymer films was characterized by measuring sample birefringence with a Babinet compensator. Birefringence Δ was determined from the relation

$$\Delta = \lambda R/t$$

where λ is the wavelength of light (in nm), R is the retardation (phase difference in wave numbers), and t is the thickness of the sample (in nm).

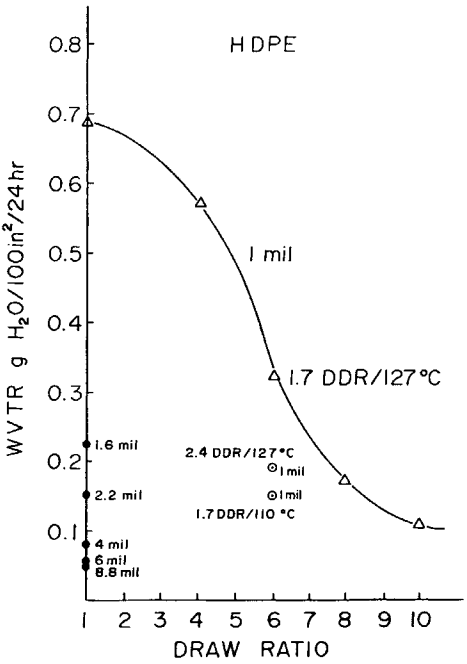

Fig. 3. Water vapor transmission rate (WVTR) as function of film draw ratio. Data are for films 1 mil thick unless otherwise labeled.

The orientation of the crystalline regions in the films was characterized using wide-angle x-ray scattering (WAXS). Transmission patterns were recorded on a flat film camera using nickel-filtered CuK_α radiation. Samples were approximately 2.54×10^{-3} cm thick, with a sample-to-x-ray film distance of 5 cm. Exposure times of 45 min were employed using a Phillips generator operated at 35 kV and 20 mA.

Barrier Measurements

Water vapor and oxygen transmission rates were determined as a function of draw ratio for the oriented high-density polyethylene samples. Oxygen transmission (O_2TR) in units of cc(S.T.P.)/100 in.^{2} 24 hr at 23°C was measured using a Modern Controls' OX-TRAN 100 instrument. Water vapor transmission (WVTR) in units of g(H_2O)/100 in.^{2} 24 hr was measured in a General Foods cabinet in which the film sample is fastened with wax over the mouth of an aluminum test dish which contains a desiccant. The dish is then placed in an atmosphere of constant temperature and humidity (38°C and 90% RH), and the weight gain of the desiccant is used to calculate the rate of water vapor transmission.

RESULTS AND DISCUSSION

Barrier Properties

Uniaxial orientation has a marked effect upon the film permeability characteristics. A plot of WVTR versus draw ratio is shown in Figure 3 for 2.5×10^{-3}-cm-thick film samples. Upon orienting the film to a draw ratio of 10×, an

80% reduction in WVTR is observed in comparison to the unoriented, as-blown film. WVTR data for unoriented (as blown, designated 1×) films of various thickness are plotted as well. It is significant to note the WVTR of a 10×10^{-3}, unoriented film is comparable to that of a 10× oriented, 2.5×10^{-3}-cm film. This improvement in water vapor permeability has economic implications in that a reduction in film gauge is possible while still retaining the barrier properties of a thicker film.

The extruded bubble orientation and postorientation temperature also have an effect upon WVTR. Increasing the extrusion drawdown ratio (DDR) (DDR ≡ die gap/BUR × film gauge, where BUR ≡ bubble diameter/die diameter) from 1.7 to 2.4 results in a 40% decrease in WVTR of otherwise identical films due to the orientation imparted to the as-blown film during its manufacture. Furthermore, over a 50% reduction in WVTR is observed when the postorientation process is conducted at 110°C instead of 127°C due to a higher degree of sample orientation retained at lower temperatures. Nakayama and Kanetsuna[9] have shown a similar relationship between amorphous orientation and orienting temperature. Peterlin[10] also has noted a greater reduction in transport properties for lower draw temperatures. A similar permeability relationship as a function of draw ratio is seen for oxygen transmission (O_2TR) in Figure 4 with almost 80% reduction on O_2TR upon drawing of 8×.

Morphology

The average degree of crystallinity determined by density and DSC methods for the as-blown film was approximately 67%. All the postoriented 4× to 10× samples had approximately the same degree of crystallinity, only slightly higher at 73% due to the combination of annealing and strain-induced crystallization during the high temperature (127°C) postdrawing process.

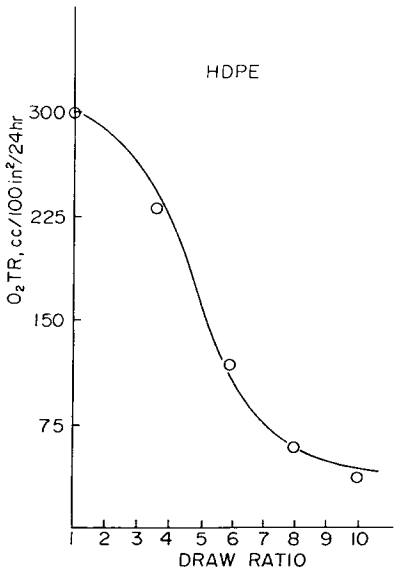

Fig. 4. Oxygen transmission rate (O_2TR) as function of film draw ratio. Data are for films 1 mil thick unless otherwise labeled.

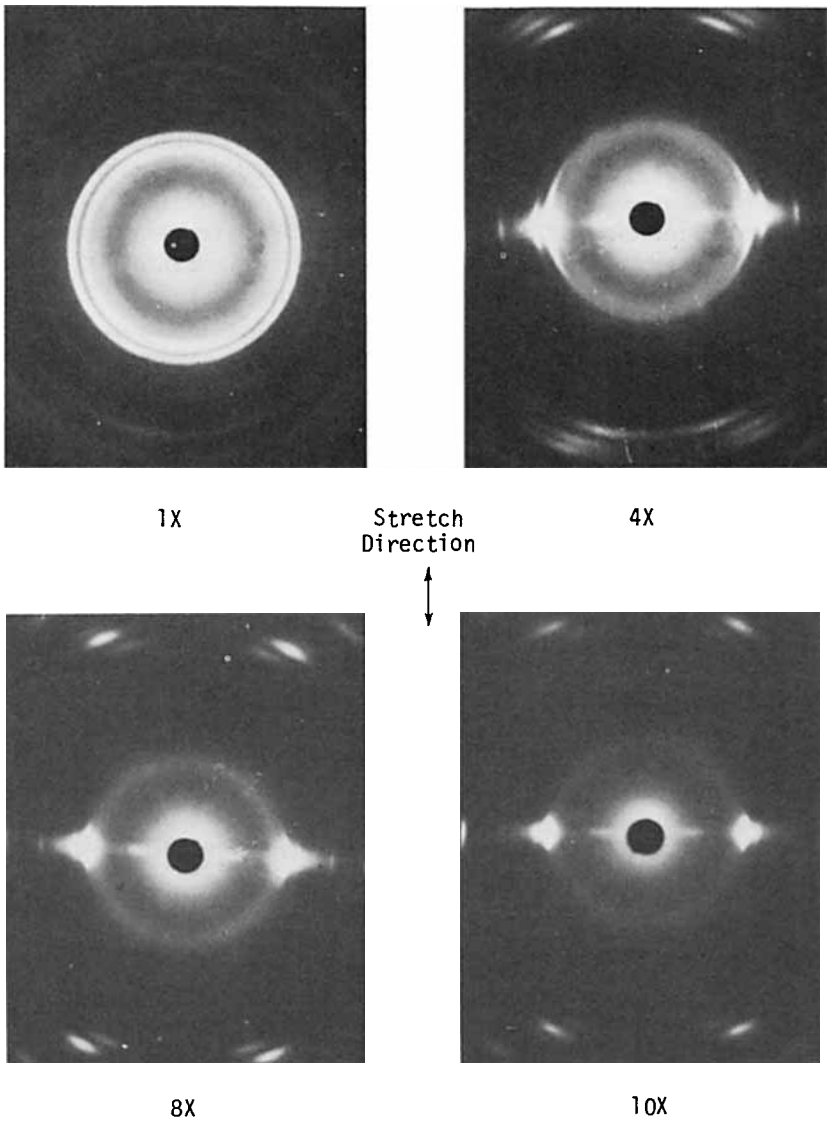

Fig. 5. Wide-angle x-ray patterns of as-blown and postdrawn films showing orientation of the crystalline phase.

Film orientation, however, is seen to increase with drawing (see Fig. 5). The texturing of the (110) reflection indicates a slight c-axis orientation during the manufacture of the as-blown film. For a film postdrawn 4×, both the (110) and (200) reflections become concentrated at the equatorial region consistent with strong chain axis alignment along the draw direction. Further drawing to 10× results in further orientation of the chain axis parallel to the stretch direction (indicated by very sharp azimuthal dependence of the (110) reflection). The diminished intensity of the (200) reflection indicates that one is achieving a "single crystal texture"[11] with the a-axis orientation normal to the c-axis and parallel to the thin dimension of the film. Film birefringence increases strongly with draw ratio as well (see Fig. 6).

The fourfold symmetrical H_v scattering pattern obtained from the as-blown polyethylene film indicates the presence of anisotropic spherulitic structure with little orientation (Fig. 7). The average size of the spherulites can be estimated by the relation derived first by Stein and Rhodes[12–14]:

$$R_0 = 4.08\lambda/4\pi \sin(\theta_m/2)$$

where R_0 = average radius of the undeformed scattering sphere, λ = wavelength of the incident light, and θ_m = scattering angle at which the scattering intensity is maximum. A wide distribution of imperfect spherulites with diameters on the order of 10 μm are present in the as-blown film.

The SALS patterns from the drawn films consist of a flattened four-lobe pattern with vertical streaks normal to the stretch direction. The intensity is maximum at the center and decreases monotonically along each of the four lobes with scattering angle. The absence of an intensity maximum at higher scattering angles and the flattened orientation of the lobes with respect to the direction of stretch suggests this scattering is from rod-like structures with their axes preferentially oriented at a small angle to the stretch direction.[15–17]

The vertical streaks normal to the stretch direction are similar to those observed by Stein and Rhodes.[18] The pair of inclined streaks in the 4× film is likely due to microfibrils partially aligned with the stretch direction, whereas the sharp single streak of the 8× and 10× films is due to a more highly aligned microfibrillar structure. Thus, a rod-like and microfibrillar morphology results from high-temperature (127°C) drawing of the originally spherulitic films.

Peterlin and Williams[8] have noted a gradual transformation of spherulitic polyethylene into a fibrous structure with increasing draw ratio at 60°C, with a subsequent decrease in film permeability. According to Peterlin, the spherulitic material is transformed into a densely packed microfibril structure which consists of folded chain crystal blocks connected in the axial direction by many extended tie molecules passing through the amorphous layers separating

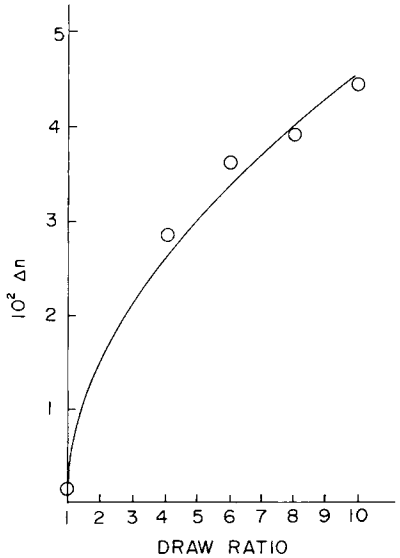

Fig. 6. Film birefringence as function of film draw ratio.

the crystal cores of adjacent blocks. This denser packing and ordering of tie molecules in the amorphous regions brought about by the drawing process and the rearrangement of both the amorphous and crystalline regions results in blocking the passage of penetrant.

Since the crystalline component is assumed impermeable, the sorption and diffusion of low molecular weight penetrant proceeds almost exclusively through the amorphous component of the semicrystalline polymer. Vapor barrier resistance thus depends upon the transport properties and geometric distribution of the amorphous regions.

The amorphous content of the films we have studied has been shown to remain relatively constant for various amounts of drawing. However, overall sample orientation does increase with increased drawing as evidenced by birefringence, WAXS, and SALS. Thus, increased orientation of the amorphous phase must account for most of the reduction in transport properties of the films.

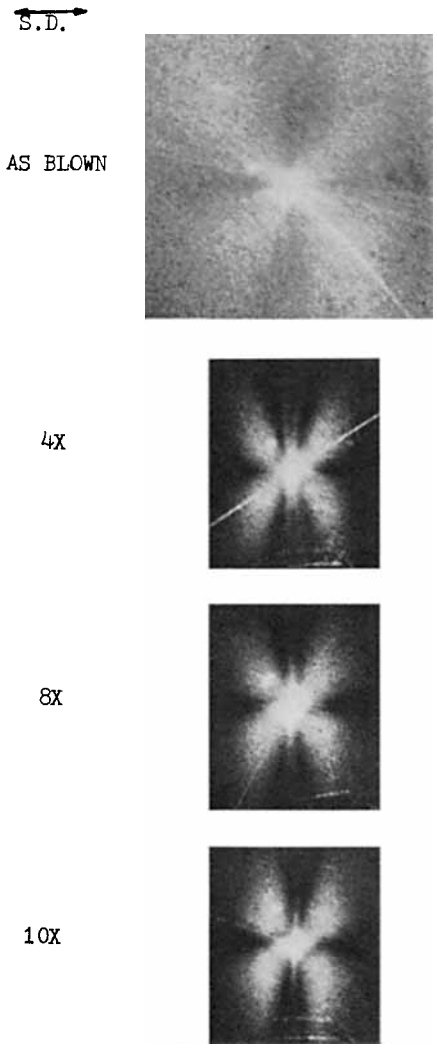

Fig. 7. Small-angle light scattering patterns of films as function of film draw ratio.

CONCLUSIONS

Transformation of an initial spherulitic superstructure to a rod-like and microfibrillar morphology has been observed in oriented linear polyethylene films with increased draw at 127°C. Crystallinity was found to be an insensitive measurement of morphological changes and correlates poorly with barrier data. Rod-like and microfibril structures oriented along the stretch direction and increased orientation of the amorphous phase are suggested to account for the decrease in transport properties with increased draw ratio.

Significantly improved barrier properties have resulted through uniaxial orientation. Moreover, further extensive microfibrillar formation and further film orientation, higher drawdown ratios, and lower orientation temperatures may bring about further barrier improvements.

This research was carried out with partial support of a University of Massachusetts Faculty Research Grant 203006.

References

1. Y. Ito, *Kobunshi Kagaku,* **18,** 6 (1961).
2. S. W. Lasoski and W. H. Cobbs, *J. Polym. Sci.,* **36,** 21 (1959).
3. A. S. Michaels and R. W. Hausselein, *J. Polym. Sci.,* **10,** 6 (1965).
4. T. E. Brady, S. A. Jabarin, and G. W. Miller, *Permeability of Plastic Films and Coatings,* H. B. Hopfenberg, Ed., Plenum, New York, 1974, p. 301.
5. W. R. Vieth, E. S. Matulevicius, and S. R. Mitchell, *Kolloid Z. Z. Polym.* **220** (1), 49 (1967).
6. Y. Ito, *Kobunshi Kagaku,* **19,** 412 (1962).
7. A. S. Michaels and H. J. Bixler, *J. Polym. Sci.,* **1,** 413 (1961).
8. J. L. Williams and A. Peterlin, *J. Polym. Sci. Polym. Phys. Ed.,* **9,** 1483 (1971).
9. K. Nakayama and H. Kanetsuna, *J. Mater. Sci.,* **10,** 1105 (1975).
10. A. Peterlin, *J. Macromolec. Sci., Phys.,* **11,** 57 (1975).
11. R. J. Young and P. B. Bowden, *J. Mater. Sci.,* **8,** 1177 (1973).
12. R. S. Stein and M. B. Rhodes, *J. Appl. Phys.,* **31,** 1873 (1960).
13. R. S. Stein, *Structure and Properties of Polymer Films, in Polymer Science and Technology,* Vol. 1, R. W. Lenz and R. S. Stein, Eds., Plenum, New York, 1973.
14. R. J. Samuels, *Structured Polymer Properties,* Wiley, New York, 1974, p. 94.
15. M. B. Rhodes and R. S. Stein, *J. Polym. Sci. Part A-2,* **7,** 1539 (1969).
16. R. J. Samuels, *J. Polym. Sci. Part A-2,* **7,** 1197 (1969).
17. T. Hashimoto, K. Nagatoshi, and H. Kawai, *Polymer,* **17,** 1063 (1976).
18. M. B. Rhodes and R. S. Stein, *J. Appl. Phys.,* **32,** 2344 (1961).

Received February 21, 1979
Revised July 30, 1979